An NMR Study of Pyridine Associated With DMPC Liposomes and Magnetically Ordered DMPC-Surfactant Mixed Micelles

Janet M. Henderson, Robert M. Iannucci, and Matthew Petersheim
Chemistry Department, Seton Hall University, South Orange, New Jersey 07079 USA

ABSTRACT With molecular dynamics simulations of phospholipid membranes becoming a reality, there is a growing need for experiments that provide the molecular details necessary to test these computational results. Pyridine is used here to explore the interaction of planar aromatic groups with the water-lipid interface of membranes. It is shown by magic angle spinning ^{13}C nuclear magnetic resonance (NMR) to bind between the glycerol and choline groups of dimyristoylphosphatidlycholine (DMPC) liposomes. The axial pattern for the ^{31}P NMR spectrum of DMPC liposomes is preserved even with more than half of the interfacial sites occupied, indicating that pyridine does not disrupt the lamellar phase of this lipid. ^{2}H NMR experiments of liposomes in deuterium oxide demonstrate that pyridine might promote greater penetration of water into restricted regions in the interface. Magnetically oriented DMPC/surfactant micelles were investigated as a means for improving resolution and sensitivity in NMR studies of species bound to bilayers. The quadrupolar splittings in the ^{2}H NMR spectra of d_5-pyridine in DMPC liposomes and magnetically oriented DMPC/Triton X-100 micelles indicate a common bound state for the two bilayer systems. The well resolved quadrupolar splittings of d_5-pyridine in oriented micelles were used to establish the tilt of the pyridine ring relative to the bilayer plane.

INTRODUCTION

Recent molecular dynamics studies provide remarkable views of the complex aqueous interface in fluid lipid membranes that are in general agreement with experimental results such as atomic order parameters for the phospholipid molecules from nuclear magnetic resonance (Paster et al., 1991; De Loof et al., 1991; Bassolino-Klimas et al., 1993; Venable et al., 1993; Xiang and Anderson, 1994). However, much of the interest in phospholipid membranes lies with the behavior of substances associating with the bilayer, e.g., membrane proteins, amphiphilic peptides, and anesthetics. The immediate possibility of now simulating this behavior (Bassolino-Klimas et al., 1993) generates a need for experimental evidence dealing with the dynamics of the included species in the membrane. Although the behavior of species in membranes has often been inferred from their effect on the phospholipid (Forrest and Mattai, 1985; Pope and Dubro, 1986; Boden et al., 1988; Boden et al., 1991; Yang et al., 1992), a complete test of simulations will require the equivalent of atomic order parameters for the included species itself.

The work presented here deals with methods for probing the behavior of small amphiphiles in the water-membrane interface. There are many classes of substances expected to partition primarily into the polar and aqueous domains of the bilayer (Sanders and Schwonek, 1993; Xiang and Anderson, 1994; Barry and Gawrisch, 1994). Depending on their size and functionality, these "probes" provide a broad range of control over the specificity of interaction with the lipid and the degree to which the species perturbs the bilayer. This is the type of control needed in experiments designed to test select details of the very complex simulations of membranes. Pyridine was chosen for these studies as an amphiphilic probe of the lipid-water interface because it is small, rigid, and aromatic, and it has three chemically distinct sites on the ring. The small size and the fact that it is not a hydrogen bond donor are features chosen to minimize the perturbation when it associates with the interface. The rigidity of the ring removes the possibility of conformational degrees of freedom in the probe, and the aromaticity can be used to locate the molecule in the membrane on the basis of ring current shifts of lipid resonances. Replacing the three chemically distinct hydrogens on pyridine with deuterons provided a convenience in determining the order parameter for the probe, which is interpreted in terms of the average orientation of the ring in the interface. Although pyridine is an ubiquitous part of our environment (Tsukioka and Murakami, 1987; Pinsky and Bose, 1988; Shimoda and Shibamoto, 1990; Kim et al., 1992; Ishihara et al., 1992; Henderson et al., 1992), there is only incidental evidence that there is biological relevance in its association with membranes (Borchard and Wolfgang, 1989; Lipnick, 1989) other than as a means for entering the cell. It is of interest here only for its properties as a probe of the interface.

As mentioned above, the aromaticity of pyridine is exploited to determine its location in the water-lipid interface through ring current shifts of the phospholipid ^{13}C resonances. In a more indirect manner, association of pyridine with the membrane can be viewed in terms of its effects on the interfacial water. Quadrupolar splitting of deuterium NMR resonances of $^{2}H_2O$ (Finer, 1973; Ulmius et al., 1977; Gawrisch et al., 1992) arises from local restrictions on the water imposed by the lipid moieties in the interface; this can be observed with multilamellar liposomes. The magnitude of

Received for publication 24 January 1994 and in final form 21 April 1994.
Address reprint requests to Matthew Petersheim, Department of Chemistry, Seton Hall University, South Orange, NJ 07079-2694. Tel.: 201-761-9029; Fax: 201-761-9772; E-mail: petersma@lanmail.shu.edu.

0006-3495/94/07/238/12 $2.00

the splitting under conditions of fast exchange reflects the fraction of molecules in locally restricted sites and the associated order parameters. Association of an amphiphile with the lipid is expected to displace some of the interfacial water and possibly alter the local environment of that which remains in the interface. The quadrupolar splitting of ^2H_2O was used in these studies to detect such changes induced by pyridine.

It was stated that pyridine was chosen in part for its small size, to minimize the local perturbation of the lipid. The ^{31}P NMR powder pattern of the phospholipid is sensitive to gross changes in the lipid phase state and was used here as a simple measure of the degree to which pyridine distorted the bilayer structure. Differential scanning calorimetry was also used to determine the degree to which pyridine perturbs the lipid and ^2H NMR of deuterated pyridine provided a measure of whether pyridine binding differs between the gel and liquid crystalline states of the bilayer.

The deuterium quadrupolar doublets can be a rich source of information for membrane-bound species such as peptides (Davis, 1988) and glycolipids (Renou et al., 1989; Sanders and Prestegard, 1991; Hare et al., 1993). There is also very little background in the ^2H spectrum from the lipid itself because of the low natural abundance for this isotope (0.015%). For pyridine and other rigid molecules, there is little need to establish structure in the membrane-bound state, but the resonance splittings can be used to characterize the orientation of the molecule relative to the bilayer normal. With liposomes the ^2H Pake peak shape spreads the resonance intensity over several kHz, incurring a dramatic decrease in sensitivity and resolution relative to the narrow resonances found in more isotropically fluid solutions. Numerical dePaking can be used to recover resolution but not sensitivity (Bloom et al., 1981). The quadrupolar doublets can be preserved while directly reducing the Pake patterns to relatively sharp resonances through the use of oriented phospholipid bilayers. This approach provides the spectral resolution generally obtained through dePaking and recovers most of the sensitivity that would be observed in a fluid isotropic solution. The second part of this work explores the use of magnetically oriented micelles for ^2H NMR studies of amphiphile behavior in the lipid bilayer.

Aqueous mixtures of several different surfactants with DMPC have been shown to form lyotropic liquid crystal phases that orient in the static magnetic field of an NMR spectrometer (Ram and Prestegard, 1988; Sanders and Prestegard, 1990, 1991, 1992; Sanders et al., 1993; Sanders, 1993). The suspensions are described as disk-shaped micelles with a DMPC bilayer as the body of the disk and the surfactant forming the rim. These micelles have been shown to orient in a magnetic field over relatively broad ranges of temperature and composition. Their principal disadvantage is that the surfactant rim and phospholipid bilayer present two micelle domains into which an analyte can partition. To establish the conditions under which pyridine associates primarily with the phospholipid domain, the micelle composition was varied by changing the surfactant/phospholipid ratio and the identity of the surfactant, using two of the systems characterized by Prestegard and Sanders: DMPC/CHAPSO and DMPC/Triton X-100 micelles.

MATERIALS AND METHODS

1,2-Dimyristoyl-*sn*-glycero-3-phosphocholine (DMPC) (>99% purity) was purchased from Avanti Polar Lipids (Alabaster, AL), Triton X-100 and 3-[(cholamidopropyl) dimethylammonio]-2-hydroxy-1-propanesulfonate (CHAPSO) from Sigma Chemical Co. (St. Louis, MO); deuterium oxide (D_2O) from Cambridge Isotope Labs (Woburn, MA) with a minimum isotopic purity of 99.9 atom% deuterium. Pyridine and pyridine-d_5 (>99.96 atom% deuterium) were purchases from J.T. Baker (Phillipsburg, NJ) and Aldrich Chemicals (Milwaukee, WI), respectively.

Sample preparation

Multilamellar vesicles with 10:1, 5:1, 1:1, and 0:1 pyridine:DMPC molar ratios and water:DMPC mole ratio constant at 56:1 were prepared for ^{13}C, ^2H and ^{31}P NMR experiments. The apparent concentration of DMPC in water is 1 M. A stock solution of pyridine in distilled water was prepared and adjusted to a pH of 9 using NaOH and HCl dilute solutions. This pH was chosen to provide aprotic pyridine to avoid electrostatic double layer effects with the partitioning into a neutral phospholipid membrane. Aliquots of this solution were added to 400-mg samples of DMPC and adjusted to 60% by weight water. All samples were capped to eliminate evaporation, and a freeze-thaw preparation was applied. Ten freeze-thaw cycles at −20°C and 80°C were completed with the samples remaining in a bath for 20-min intervals. A 1:1 d_5-pyridine:DMPC sample was similarly prepared for deuterium NMR analysis. To obtain deuterium NMR spectra of the water associated with the membrane, samples with the four pyridine:DMPC ratios were again prepared using D_2O.

Surfactant/DMPC micelles, where the surfactant is either CHAPSO or Triton X-100, were prepared by weighing the appropriate amounts of surfactant, DMPC, d_5-pyridine, and 0.1 M sodium phosphate buffer, pH 9.0, directly into a 5 mm NMR tube. The samples were then heated to 40°C in a water bath and centrifuged at low rpm for 15–20 min. A glass rod was then used to further mix the sample after warming to 40°C followed by additional centrifuging at low rpm. This cycle was repeated 4–5 times until the sample became clear, indicating micelle formation.

Instrumentation

All NMR spectra with multilamellar suspensions were acquired on a Varian VXR-300 spectrometer having a magnetic field strength of 7.05 Tesla. This system is equipped with a multinuclear Doty solids probe and variable temperature unit. ^{31}P and ^2H spectra were collected with the rotor fixed in place, to preserve the powder patterns, using a Hahn-echo pulse sequence. ^{13}C spectra were obtained with magic angle spinning (MAS) at 2 kHz, and both ^{31}P and ^{13}C spectra were collected with proton decoupling. NMR experiments with DMPC/surfactant micelles were performed on a General Electric QE-300 NMR spectrometer, also at 7.05 Tesla, equipped with broad band capabilities and a 5 mm $^1H/^{13}C$ dual probe. ^2H spectra were collected through the lock coil, and ^{13}C spectra of magnetically oriented samples were collected with broad band decoupling. Experiments were performed at 40°C unless otherwise indicated.

Differential scanning calorimetry (DSC) data were obtained with a Seiko Instruments Model 220C equipped with an auto cooling unit. Samples prepared by the freeze-thaw cycles described above were weighed into aluminum pans with lids using a microbalance, cooled from room temperature to 0°C at 30°C/min, held for 10 min at 0°C, and heating thermograms were collected from 0 to 50°C at 1°C/min using an air reference.

RESULTS

Studies with multilamellar liposomes

^{13}C NMR studies: pyridine localizes in the interface

Liposome suspensions give rise to broad, poorly resolved ^{13}C NMR peaks because the tumbling motion of the liposome assembly is too slow to average the chemical shift anisotropies. These broad powder patterns can be artificially narrowed by way of magic angle spinning, providing resolved resonances for most chemically distinct carbons in the lipid. Addition of pyridine to a DMPC suspension results in upfield shifts of nearly all of these ^{13}C resonances (Table 1). Note that the entries in Table 1 are ordered according to decreasing pyridine-induced shifts at 10:1 pyridine:DMPC. The shifts are greatest for the head group glycerol carbons, but the changes are not monotonic with distance from the interface. These observations suggest that the pyridine has a preferred orientation in the membrane and is sandwiched between the choline and glycerol moieties. The small shifts of the fatty acid resonances support the expectation that the pyridine permeates the hydrophobic domain to a lesser extent.

These ring current shifts are the clearest NMR measures of intermolecular contacts besides direct dipolar coupling, often exploited as the nuclear Overhauser effect. Both tools are of great potential use in testing membrane simulations. Some caution must be taken in interpreting the relative magnitudes of the shifts because they will vary as $-\langle(3\cos^2\xi - 1)/r^3\rangle$, where ξ defines the position of the atom relative to the ring's normal and r is the distance to the center of the pyridine ring. The average indicated by the brackets would involve all phospholipid molecules close to the pyridine and their fluctuations. This averaging necessarily requires the molecular details of a dynamic simulation. The fact that the choline and glycerol resonances exhibit the largest upfield shifts suggests that these groups are close to the faces of the ring, on average, which is consistent with the interfacial binding of benzyl alcohol suggested by Boden et al. (1988).

Adsorption coefficient for pyridine binding to DMPC

Because pyridine appears to bind primarily in the interface, it is reasonable to treat the binding as a simple adsorption equilibrium. It will be assumed that the surface concentration of sites equals the surface concentration of lipid headgroups with no nearest-neighbor exclusion. This yields an apparent adsorption coefficient of the form

$$K_{app} = f/\{([P]_t - f[S]_t)(1 - f)\}, \quad (1)$$

where f is the fraction of surface sites occupied by pyridine, $[P]_t$ the total molar pyridine concentration in absence of the lipid, and $[S]_t$ is the apparent molar concentration of binding sites, which is the apparent molar concentration of DMPC in this model. The pyridine is in fast chemical exchange with

TABLE 1 ^{13}C MAS-NMR Resonances and ^2H_2O quadrupolar splittings for multilamellar DMPC with pyridine at pH 9, 40°C: calculated fraction bound and the apparent adsorption coefficient for pyridine

Pyridine/DMPC[a]	0/1 δ(ppm)[b]	1/1 $\Delta\delta_1$[c]	5/1 $\Delta\delta_5$[c]	10/1 $\Delta\delta_{10}$[c]	$\Delta\delta_{sat}$[d]	f_1[e]	f_5[e]	f_{10}[e]	K_{app}[e]
Glycerol *sn*-2	71.43	−0.19	−0.6	−0.73	−0.91	0.21	0.66	0.81	0.34
Choline N-CH_3	54.73	−0.16	−0.56	−0.72	−0.97	0.16	0.57	0.74	0.23
Choline CH_2-N	66.7	−0.11	−0.41	−0.6	−1.08	0.10	0.38	0.56	0.13
Choline N-CH_3	54.73	−0.16	−0.35	−0.51	−0.91	0.18	0.39	0.56	0.26
Glycerol *sn*-1	63.48	−0.03	−0.3	−0.48	−1.16	0.03	0.26	0.41	0.03
Acyl α-CH_2	34.39	−0.08	−0.29	−0.42	−0.73	0.11	0.39	0.57	0.14
Acyl β-CH_2	25.18	−0.14	−0.32	−0.34	−0.36	0.39	0.89	0.95	1.05
Choline O-CH_2	59.73	−0.05	−0.21	−0.31	−0.57	0.09[g]	0.37[g]	0.54[g]	0.11[g]
Glycerol *sn*-3	63.98	0.02	−0.13	−0.24	−1.54	−0.01[g]	0.08[g]	0.16[g]	−0.01[g]
Acyl CH_2s	30.01	−0.08	−0.18	−0.16	−0.15	0.54[g]	1.22[g]	1.08[g]	2.57[g]
Carbonyl	173.52	0.07	−0.07	−0.16	0.58	0.12	−0.12[g]	−0.28[g]	0.16[g]
(ω-2)-CH_2	32.09	−0.04	−0.12	−0.14	−0.16	0.24	0.73	0.85	0.43
(ω-1)-CH_2	22.7	−0.02	−0.08	−0.09	−0.10	0.20	0.79	0.89	0.31
Acyl CH_3	13.8	0	0	0					
Average[h] =						0.17	0.54	0.69	0.30
(95% conf. int.)[h]						(±0.07)	(±0.12)	(±0.10)	(±0.16)
D_2O $\Delta\nu_\alpha$ (Hz)[i]	327	389	595	691	874	0.11	0.49	0.67	0.13

^{13}C Resonances Listed According to Pyridine-Induced Shifts.

[a] Pyridine to DMPC mole ratio.

[b] ^{13}C chemical shift with the fatty acid methyl resonance set to 13.80 ppm. Resonances are listed in order of decreasing pyridine-induced shift.

[c] Change in chemical shift relative to DMPC alone.

[d] Chemical shift change for a surface saturated with pyridine, calculated from Eq. 3.

[e] Fraction of surface sites occupied with 10:1 (f_{10}), 5:1 (f_5) and 1:1 (f_1) pyridine:DMPC sample, calculated from the changes in chemical shift and Eq. 2. K_{app}: apparent adsorption coefficient (M^{-1}) calculated from the values for f_1 and Eq. 1 using 1 M for the total concentration of pyridine and the binding sites, each.

[g] These quantitites were excluded from the averages because one or more values calculated from the shifts of this resonance was physically meaningless, i.e., negative or values for f greater than one.

[h] Averages and 95% confidence intervals calculated excluding the values labeled. Values were rejected if one of the quantities calculated from that resonance was physically meaningless, e.g., fractions greater than unity or less than zero, or negative adsorption coefficients.

[i] Observed quadrupolar splittings of ^2H_2O and the corresponding quantities calculated from these splittings.

the surface sites (vide infra), and so in this simple model the fraction of surface sites occupied can be estimated from any of the NMR observables as

$$f = \Delta y_{obs}/\Delta y_{sat}, \quad (2)$$

where Δy_{obs} is the observed change in a parameter relative to the system with no pyridine and Δy_{sat} is the change expected for a surface saturated with pyridine ($f = 1$). None of the experiments presented yield definitively saturated lattices, consequently it was necessary to estimate values of Δy_{sat} in the following manner. Given that the apparent site concentration, $[S]_t$, was the same for all levels of pyridine, Eqs. 1 and 2 can be rearranged, using the values for two different pyridine concentrations, to yield a quadratic in Δy_{sat},

$$(r_1/\Delta y_1 - r_2/\Delta y_2)(\Delta y_{sat})^2 - (r_1 - r_2)\Delta y_{sat} + (\Delta y_1 - \Delta y_2) = 0, \quad (3)$$

where r_1 and r_2 are the two pyridine to DMPC mole ratios and Δy_1 and Δy_2 are the corresponding changes in the observable, e.g., chemical shift or quadrupolar coupling. Table 1 contains values of $\Delta\delta_{sat}$ calculated from Eq. 3 using the DMPC ^{13}C resonances for 5:1 and 10:1 pyridine:DMPC. The fraction of sites occupied at all three levels of pyridine are also given in the table, and the apparent partition coefficient was calculated from the fraction occupied at 1:1 pyridine:DMPC using Eq. 1.

Differential scanning calorimetry: confirmation of interfacial binding

Fully hydrated DMPC exhibits two thermotropic transitions: near 15°C there is a change from $L_{\beta'}$ (lamellar gel phase) to $P_{\beta'}$ (ripple phase), referred to as the pretransition, and the main transition near 25°C corresponds to the change from ripple phase to the liquid crystalline phase (L_α) (Cevc, 1991). DSC thermograms for DMPC and 1:1 pyridine:DMPC in ^2H_2O are given in Fig. 1. Pyridine induces a decrease in the pre-transition enthalpy and peak temperature, which are common effects of substances partitioning into the lipid (Mountcastle et al., 1978; Makriyannis et al., 1986; Gaillard et al., 1991). The main transition exhibits a smaller decrease in peak temperature and actually increased in enthalpy with the addition of pyridine. The increase in enthalpy for the main transition is similar to that observed by Boden et al. (1988) for binding of benzyl alcohol. They interpreted this increase as evidence for displacement of the alcohol from the interface upon forming the gel state. The excess enthalpy was attributed to solvation of the free benzyl alcohol.

Pyridine also has opposite effects on the widths of the two transitions, causing the main transition to become narrower and broadening the pre-transition (Fig. 1). According to the Monte Carlo simulations by Jørgensen et al. (1993), this behavior of the main transition is indicative of an amphiphile that does not intercalate into the acyl chain domain and, to some extent, is displaced from the bilayer upon forming the gel state. Species that are not readily displaced cause a broadening of the transition and a drop in T_m (Jørgensen et al., 1993), as observed for the pre-transition.

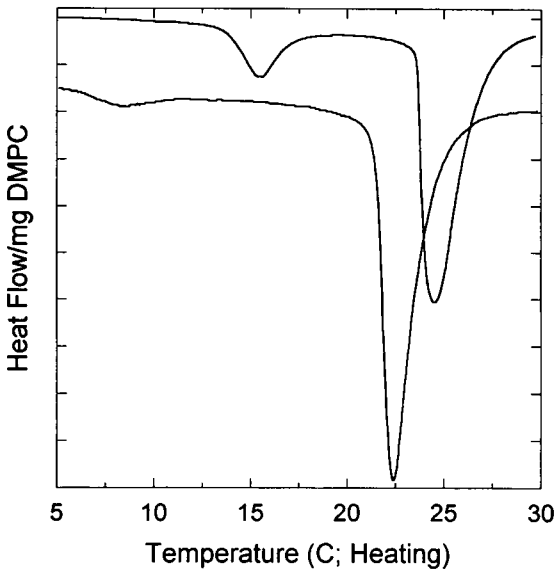

FIGURE 1 Differential scanning calorimetry heating thermograms for DMPC liposomes and liposomes with 1:1 pyridine:DMPC, pH 9.0, in ^2H_2O. DMPC liposomes with no pyridine (*top*) exhibit a main transition ($P_{\beta'} \rightarrow L_\alpha$) with a maximum at 24.4°C, an area of 29 kJ/mole and a width at half height of 2°C. The pretransition ($L_{\beta'} \rightarrow P_{\beta'}$) was located at 15.5°C with an area of 4.3 kJ/mole and a 2°C width. Use of deuterium oxide instead of water in these studies might account for the small differences between these values and those reported by Mabrey and Sturtevant (1976), i.e., a main transition with an enthalpy of 22.6 kJ/mole at 23.9°C and the pretransition of 4.2 kJ/mole at 14.2°C. In the presence of 1:1 pyridine:DMPC (*bottom*), the main transition increases to 34 kJ/mole but drops to 22.6°C with a width of 1.7°C, and the pretransition decreases to 1.7 kJ/mole, drops to 8.6°C, and increases in width to 4°C.

^{31}P NMR: virtually no perturbation of the phosphodiester by pyridine

The ^{31}P powder pattern provides a simple measure of changes in the local dynamics of the phosphodiester moiety and the motions of the molecules and membrane as a whole (Seelig, 1978; Watts and Spooner, 1991). Changes in shape of this resonance can be used as measures of the extent to which an adsorbate perturbs the phase properties of the lipid membrane. At 40°C DMPC is in the liquid crystalline state and exhibits an axial powder pattern with an averaged shielding anisotropy of 45–46 ppm (Seelig, 1978; Gaillard et al., 1991). Adsorption of pyridine results in only subtle changes in the resonance shape (Fig. 2) with no measurable change in the anisotropy and little change in the second moment of the resonance even with up to 70% of the surface sites occupied (Table 1). Consequently, pyridine must not significantly alter the packing and dynamics of the phosphodiester moieties.

^2H NMR of ^2H_2O: tightly bound water is not displaced by pyridine

Molecular dynamics simulations of phospholipid bilayers clearly show motionally restricted water molecules associ-

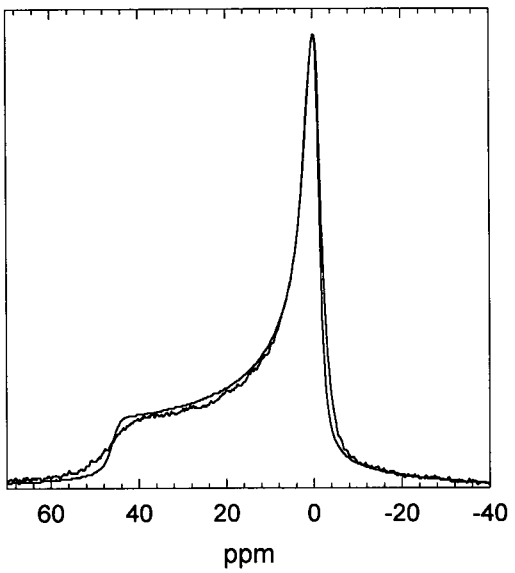

FIGURE 2 121 MHz ^{31}P NMR powder pattern spectra for DMPC liposomes (30% w/w water) at pH 9 and 40°C. Spectra for DMPC alone and that for 10:1 pyridine:DMPC (the noisier of the two) are overlapped to emphasize that the pyridine has very little effect on the shape of the resonance.

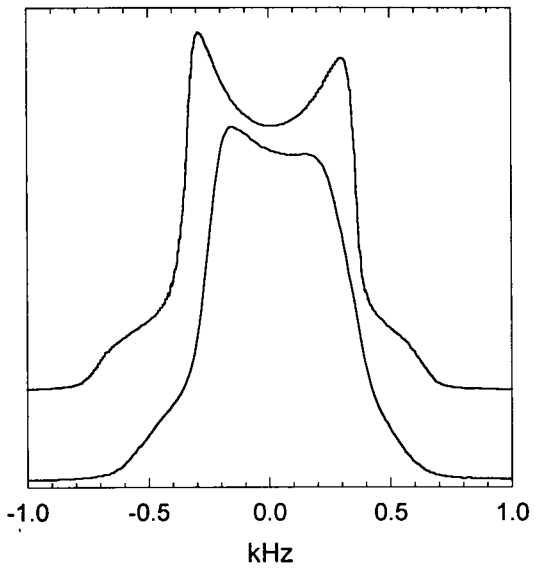

FIGURE 3 46 MHz ^{2}H NMR powder pattern spectra of $^{2}H_2O$ in DMPC liposomes (30% w/w water) with 5:1 pyridine:DMPC (*top*) and without pyridine (*bottom*) at pH 9 and 40°C. Pyridine causes an increase in quadrupolar splitting of the $^{2}H_2O$ resonance, suggesting that the tightly bound water in the interface is not displaced by adsorption of the pyridine.

ated with the headgroup and glycerol ester groups, and occasional penetration of water clusters deeper into the hydrophobic center (De Loof et al., 1991; Bassolino-Klimas et al., 1993; Venable et al., 1993; Xiang and Anderson, 1994). The deuterium NMR spectrum of $^{2}H_2O$ with multilamellar liposomes gives evidence of this restricting environment for water. Anisotropic averaging of the deuterium quadrupolar coupling results in the single ^{2}H resonance for $^{2}H_2O$ splitting into Pake doublets (Finer, 1973; Ulmius, 1977; Gawrisch et al., 1992). Fig. 3 shows this resonance splitting for $^{2}H_2O$ in the presence of DMPC liposomes with and without pyridine. The $^{2}H_2O$ to DMPC mole ratio was 56:1 for all of the samples studied, and the temperature was 40°C.

The interfacial water molecules are in rapid exchange with the "bulk" water between the bilayers of multilamellar liposomes. As a result, the observed quadrupolar splitting is a population-weighted average of splittings from the various interfacial states and zero splitting from water that is tumbling isotropically between the bilayers. The extent of this averaging is substantial given that polycrystalline $^{2}H_2O$ ice exhibits a resonance splitting of approximately 170 kHz (Finer, 1973), and the largest reported splittings for $^{2}H_2O$ associated with phospholipids in the liquid crystalline state are on the order of 2 kHz (Finer, 1973; Ulmius, 1977; Gawrisch et al., 1992). A single narrow resonance can be observed superimposed on the Pake patterns if there is an excess of water outside of the liposome or lipid assemblies that behave isotropically on the NMR timescale, e.g., cubic phases. Because water between the bilayers tumbles almost isotropically, contributing zero splitting to the average, the magnitude of the observed quadrupolar splitting depends strongly on the water/lipid mole ratio (Finer, 1973; Ulmius, 1977; Gawrisch et al., 1992). There is also a strong dependence on phase state of the lipid, with fewer water molecules bound in the gel state than the liquid crystalline state, and temperature, which affects the local motions available in the gel state and the amount of water penetrating into the interface in the liquid crystalline state.

The resonance splitting increases slightly with increasing pyridine (Table 1). This is the opposite of what might be expected if pyridine displaces the motionally restricted water in the interface when it associates with the glycerol and choline moieties, as suggested by the ^{13}C spectra. The fact that the $^{2}H_2O$ splitting does not decrease when pyridine binds indicates that the water molecules displaced from between the glycerol and choline moieties must behave nearly isotropically in that environment, contributing little to the observed deuterium splitting even in the absence of pyridine. This interpretation could be tested by analyzing the motions of interfacial water molecules in simulations, although current approaches would not include exchange of protons (deuterons) among water molecules, which will contribute to the apparent isotropic character of the water.

The increase in $^{2}H_2O$ quadrupolar splitting when pyridine is added suggests that either the pyridine further restricts the motion of the water responsible for the quadrupolar splittings or it promotes the penetration of water into the restricted environments by altering the lipid packing. There is insufficient evidence to distinguish these two possibilities. The decrease in transition temperature in the DSC thermograms supports a pyridine-induced change in acyl chain packing, but the insensitivity of the ^{31}P powder pattern to pyridine indicates that the changes in packing must be subtle. Although it is tempting to discuss site-specific binding of the

water molecules and the effect of pyridine on this binding, the complexity of the interface depicted by dynamics simulations leads to a very ambiguous definition of these sites in a fluid membrane.

Equations 1–3 were also applied to ^2H_2O quadrupolar splittings to estimate the pyridine adsorption coefficient (Table 1). $\Delta\nu_{sat}$ from the 5:1 and 10:1 data was estimated as 874 Hz, and the fraction of the pyridine bound and the adsorption coefficient calculated from this value are in very good agreement with those from the ^{13}C data (Table 1). This supports the supposition that the quadrupolar splitting changes in direct response to the level of bound pyridine and is not some indirect effect caused by the unbound pyridine, e.g., changes in hydration or the hydration forces due to the excess pyridine between bilayers.

^2H NMR of d_5-pyridine: pyridine is bound to gel and liquid crystalline states

Deuterium NMR experiments with d_5-pyridine provides the means to test whether pyridine is displaced from the interface in the gel state, as suggested by the DSC studies. An example of the axial powder pattern observed with d_5-pyridine binding to multilamellar liposomes is given in Fig. 4. Note that there is no evidence of an isotropic resonance, indicating fast exchange of free and bound pyridine at all temperatures studied.

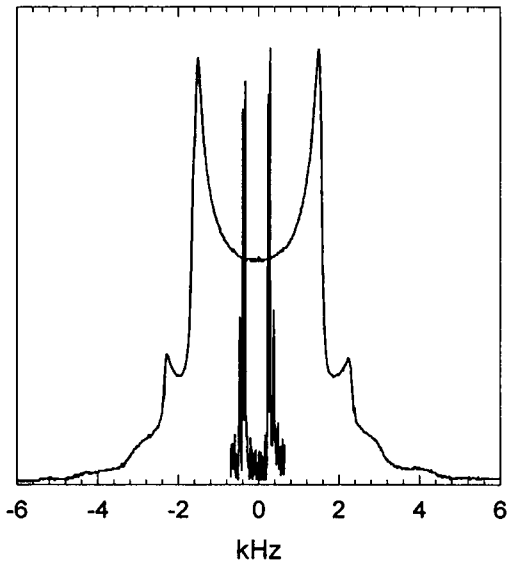

FIGURE 4 46 MHz ^2H NMR spectra of 1:1 d_5-pyridine:DMPC in a multilamellar liposome suspension (*powder pattern*) and oriented micelles consisting of 4:1 DMPC:CHAPSO (*high resolution spectrum*) at pH 9 and 40°C. The powder pattern spectrum was acquired on a 7 mm solenoid solids probe tuned to ^2H, whereas the high resolution spectrum was collected through the lock coil of a 5 mm high resolution $^1H/^{13}C$ probe. Consequently, the relative signal-to-noise levels in the two spectra reflect the sensitivity of the two different types of coil. The resonances for the oriented sample are approximately 20 Hz full width at half maximum. $\Delta\nu_\perp(o, m)$, the quadrupolar splitting for the unresolved ortho and meta doublets, is the frequency difference between the two tallest features in both spectra, and the next tallest features correspond to $\Delta\nu_\perp(p)$.

At the level of pyridine in this sample, the main transition for DMPC should fall between 20 and 30°C. Displacement of pyridine upon forming the gel state should result in a dramatic drop in the observed quadrupolar splitting. Instead, there is actually a slight increase in this temperature range (Table 2). There is also a dramatic increase in the splitting when the temperature is dropped to 10°C. Consequently, if pyridine is displaced during the main transition, as suggested by the DSC studies, there must be a very substantial fraction of the pyridine still bound in the gel state. The magnitude of the quadrupolar splittings is very likely increasing as the temperature is lowered because of greater order imposed on the pyridine remaining bound. There may be a contribution from a change in the average orientation relative to the bilayer normal as indicated by a change in the ratio of the ortho and meta splittings with the para splitting (Table 2).

The order parameter for the pyridine molecular director in the bilayer, S_D, can be estimated from these results using the fraction of pyridine bound calculated from the ^{13}C and ^2H_2O data. For 1:1 pyridine:DMPC at 40°C, the fraction of surface sites occupied is 0.17 ± 0.07 (Table 1), which is also the fraction of the total pyridine bound at this ratio. The quadrupolar splittings for the para deuterons can be expressed in terms of fraction bound and the molecular order parameter for bound pyridine as

$$\Delta\nu_\perp(p) = -3Af S_D/4. \quad (4)$$

Using 185 kHz for A (Abe and Yamazaki, 1989) and given that the sign on the resonance splitting is not known, $S_D = \pm 0.20$ (± 0.08).

Studies with magnetically oriented DMPC/surfactant micelles

NMR experiments with magnetically oriented phospholipid/surfactant micelles retain the rich structural information inherent in quadrupolar coupling, dipolar coupling, and chemical shift anisotropy while providing a dramatic improvement in sensitivity and spectral resolution over equivalent experiments with liposome suspensions (Sanders and Prestegard, 1990; Sanders, 1993; Sanders et al., 1993). Sample preparation and instrumental demands are both simpler with the micelle systems than the alternatives for NMR studies of species bound to membranes. The principal disadvantage

TABLE 2 Quadrupolar splitting for d_5-Pyridine in DMPC multilamellar liposomes as a function of temperature

T (°C)	$\Delta\nu_\perp(o, m)^a$ (kHz)	$\Delta\nu_\perp(p)^a$ (kHz)	$\Delta\nu_\perp(o, m)/\Delta\nu_\perp(p)$
10	5.009	7.877	0.636
20	3.759	4.815	0.781
30	3.448	4.684	0.736
40	3.186	4.590	0.694
50	3.018	4.521	0.668

[a] Magnitude of the splitting for the component of the quadrupole moment perpendicular to the applied field: $\Delta\nu_\perp(o, m)$ for the unresolved ortho and meta resonances and $\Delta\nu_\perp(p)$ for the para deuteron.

with these micelles comes from the presence of the surfactant. Although the DMPC is present in a bilayer assembly, the surfactant forms a nonbilayer domain that presents a second environment for substances bound to the micelle. Conditions under which the model amphiphile, pyridine, binds primarily to the DMPC domains are given in the following sections along with an analysis of the average orientation of pyridine in these domains.

^2H NMR spectra of d_5-pyridine: liposomes versus oriented micelles

Fig. 4 demonstrates the dramatic improvement in resolution of the d_5-pyridine quadrupolar splittings in going from DMPC liposomes to oriented DMPC/surfactant micelles. A direct comparison of sensitivity is not reasonable with these two spectra because two different probes were used. The spectrum with the liposomes was collected using a 7 mm solenoid coil tuned to deuterium, whereas that for the oriented spectrum was collected with a 5 mm high resolution probe using the deuterium lock coil. Assignment of the para resonances can be made on the basis of relative amplitude. In a ^1H NMR spectrum, the meta and ortho resonances can be distinguished by their scalar coupling patterns, but ^2H-^2H scalar couplings are too small to be resolved clearly with these samples. Assignments of the meta and ortho resonances were made here using the known chemical shifts for aprotic pyridine, 8.5, 7.9, and 7.5 ppm for ortho, para, and meta, respectively, and the fact that the doublets are observed to be symmetric about the original resonances. This is shown in Fig. 5 for a sample that is not completely mixed. There are two coexisting micelle phases present, one that does not orient in the field, which is represented by the three pyridine resonances in the center of the spectrum, and an oriented phase, indicated by the doublets split about the center. The lines indicate the symmetric splitting. It should be noted that the doublet centers could have been distorted away from the positions of the isotropic resonances as a consequence of chemical shift anisotropy from the pyridine ring current. The symmetric splitting observed in Fig. 5, and the overall self-consistency of the assignments we made, indicate that the chemical shifts are not appreciably different in the oriented and unoriented phases. More general approaches to assigning the split resonances in complex situations may require either selective deuteration or deuterium-carbon heterocorrelation experiments.

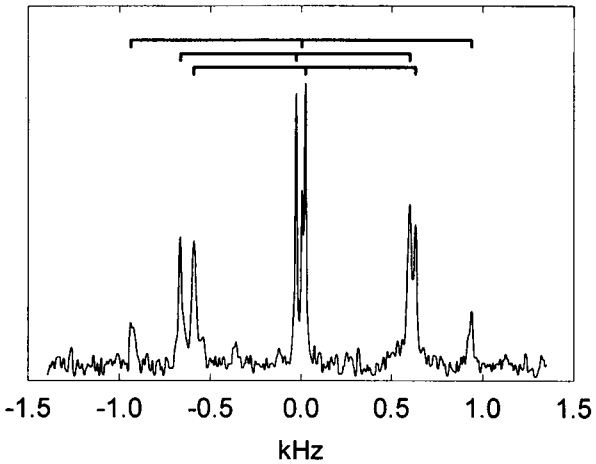

FIGURE 5 Resonance assignments for ^2H NMR spectrum of d_5-pyridine in coexisting oriented and isotropic phases. The sample is 1:1 pyridine: DMPC in a 4:1 DMPC:Triton X-100 suspension that is not fully mixed. The three peaks in the center of the spectrum are for d_5-pyridine in an isotropic micelle phase and the doublet wings about the center are for d_5-pyridine in an oriented phase; both sets of resonances are observed because of slow diffusive exchange between the two bulk phases. Solid lines above the spectrum indicate the symmetric placement of the doublets about each of the three isotropic peaks. The assignments for the three center peaks are ortho, para, and meta, from left to right, based on the known relative chemical shifts for these three ring positions.

Effects of micelle composition: pyridine partitioning into surfactant versus DMPC domain

In the simplest view of these micelles, pyridine can be considered as partitioning among three phrases: bulk aqueous, DMPC bilayer, and the nonbilayer surfactant domain. Because only three quadrupolar doublets are observed, this partitioning must occur in the fast exchange regime.

To test whether there is binding of pyridine to the surfactant domain, micelles were prepared with several DMPC/surfactant ratios and two different surfactants: CHAPSO and Triton X-100. Tables 3 and 4 show that the magnitude of the quadrupolar splitting increases with the DMPC/surfactant ratio, holding the water content constant at 65% by weight. The increase for the Triton X-100 samples is slight compared with that of CHAPSO. These trends with increasing DMPC/surfactant ratio can be caused by a combination of factors: an increase in the fraction of the pyridine binding to DMPC, an increase in total bound pyridine, and an increase in the liquid crystal order parameter. The last two can be factored from the trends by considering ratios of ortho, meta, and para splittings (vide infra). Any remaining dependence on micelle composition will reflect a shift in partitioning between the DMPC and surfactant domains.

The splitting ratios in Table 3 change with the DMPC/CHAPSO ratio, indicating that the pyridine does partition into both the DMPC and surfactant domains when CHAPSO is used. Pyridine appears to bind to only one of the domains with the DMPC/Triton X-100 micelles (Table 4) because the ratios of splittings are relatively invariant with DMPC content. Both data sets appear to approach the same ratios of

TABLE 3 D_5-pyridine quadrupolar splittings in DMPC/CHAPSO micelles, 65% w/w water, pH 9, 40°C

(DMPC[a]/CHAPSO)	$\Delta\nu_o$ (kHz)	$\Delta\nu_m$ (kHz)	$\Delta\nu_p$ (kHz)	R_{op}[b]	R_{mp}[b]
3/1	0.240	0.241	0.292	0.822	0.825
4/1	0.465	0.460	0.596	0.780	0.772
5/1	0.986	0.974	1.288	0.766	0.756
7/1	1.320	1.301	1.870	0.706	0.696

[a] Mole ratio; d_5-pyridine:DMPC 1:1 mole ratio for all samples.
[b] $R_{op} = \Delta\nu_o/\Delta\nu_p$ and $R_{mp} = \Delta\nu_m/\Delta\nu_p$.

TABLE 4 Quadrupolar splittings and micelle order parameters for d_5-pyridine in DMPC/triton X-100 micelles, 65% w/w water, pH 9, 40°C

(Pyridine[a]/DMPC)	(DMPC[a]/Triton X)	$\Delta\nu(o)$ (kHz)	$\Delta\nu(m)$ (kHz)	$\Delta\nu(p)$ (kHz)	R_{op}	R_{mp}	$\Delta\delta$(CO1)[b] (ppm)	S_γ[c]
1/1	3/1	1.17 ± 0.05	1.17 ± 0.05	1.83 ± 0.03	0.640	0.640	−8.74	0.857
2/1	3/1	1.23 ± 0.01	1.18 ± 0.01	1.84 ± 0.01	0.668	0.642		
1/1	4/1	1.29 ± 0.01	1.24 ± 0.01	1.87 ± 0.01	0.690	0.662	−8.77	0.860
2/1	4/1	1.29 ± 0.01	1.25 ± 0.01	1.88 ± 0.01	0.685	0.665		
1/1	5/1	1.34 ± 0.05	1.27 ± 0.05	1.95 ± 0.05	0.676	0.641	−9.18	0.900
2/1	5/1	1.30 ± 0.01	1.26 ± 0.01	1.89 ± 0.01	0.688	0.664		
1/1	7/1	1.30 ± 0.07	1.30 ± 0.07	2.03 ± 0.05	0.640	0.640	−9.22	0.904

[a] Mole ratios.
[b] Chemical shift difference for the *sn*-1 carbonyl ^{13}C NMR: δ(oriented sample) − δ(liposomes). Both chemical shifts are referenced to the terminal methyl group of the myristoyl chain and the spectrum for the multilamellar liposome samples was collected using magic angle spinning.
[c] Calculated from Eq. 9.

splittings with increasing DMPC and, in fact, are approaching the values observed for d_5-pyridine binding to DMPC liposomes at 40°C (Table 2). These observations provide strong evidence that, in the DMPC/Triton X-100 micelles, pyridine binds primarily to the phospholipid domain.

^{13}C NMR of the oriented micelles: estimating the micelle order parameter

The order parameter for the micelles, S_γ, can be estimated from the changes in ^{31}P or ^{13}C chemical shifts for the phospholipid in going from isotropic to oriented states (Sanders, 1993). However, with pyridine bound to the micelles, the lipid resonances can shift not only as a result of magnetic ordering, but also the average proximity of the atom to the pyridine ring. Of the DMPC ^{13}C resonances characterized by Sanders (1993), two exhibit relatively large shifts due to ordering with only small shifts due to the binding of pyridine (Table 1): the *sn*-1 carbonyl of DMPC (CO1) and the terminal methyl of the myristoyl chain (C14). Assuming the effect of pyridine on these resonances is negligible and given that the C14 resonance is used as a chemical shift reference in all spectra, the micelle order parameter can be estimated from

$$S_\gamma = \Delta\delta(\mathrm{CO1})_{obs}/\{\Delta\delta(\mathrm{CO1})_{max} - \Delta\delta(\mathrm{C14})_{max}\}, \quad (5)$$

where $\Delta\delta$ is the change in chemical shift relative to the unoriented spectrum and the subscripts refer to the observed shift and the maximum shifts expected for perfectly oriented micelles. For DMPC/Triton X-100 micelles Sanders (1993) estimated $\Delta\delta_{max}$ to be −8.4 for CO1 and 1.8 ppm for C14. Table 4 lists experimental values for $\Delta\delta(\mathrm{CO1})_{obs}$ and the corresponding values of S_γ.

Fraction pyridine binding to the DMPC/Triton X-100 micelles

It is reasonable to assume that pyridine has the same value for S_D in the DMPC/Triton X-100 micelles as it does in the DMPC liposomes given that the d_5-pyridine splitting ratios are the same (Tables 2 and 4). Using this S_D from the liposome studies (±0.20) and the values of S_γ from the ^{13}C chemical shifts, the para-deuteron splittings yield $f = 0.08 \pm 0.03$ for the fraction of pyridine bound to the DMPC/Triton X-100 micelles (Eq. 4a). This is roughly half the value expected from the DMPC liposome studies with similar pyridine and DMPC concentrations, i.e., $f = 0.17 \pm 0.07$. An underlying assumption in this analysis is that all micelles to which pyridine binds are oriented. The values for S_γ are very close to unity, indicating that most of the DMPC is incorporated into oriented micelles. However, it is reasonable to assume that some of the Triton X-100 forms micelles that are relatively free of DMPC. These could be closer to spherical in shape and unoriented. Therefore, the total pyridine bound to micelles could be greater than that indicated by the ^{2}H splittings.

Relation between ^{2}H resonance splittings for d_5-pyridine and its orientation in the bilayers

Assuming the quadrupolar coupling for the deuterons of pyridine is axially symmetric about the carbon-deuteron bond, the quadrupolar splitting of resonance i for pyridine in fast exchange between a free and micelle bound state is given as (Murari et al., 1986; Sanders and Prestegard, 1990)

$$\Delta\nu_{qi} = 3Af\tfrac{1}{2}\langle 3\cos^2\gamma - 1\rangle\tfrac{1}{2}\langle 3\cos^2\alpha_i - 1\rangle/2, \quad (6)$$

where A is the electric quadrupole coupling constant, which is on the order of 180–190 kHz for aromatic deuterons (Abe and Yamazaki, 1989), f is the fraction of pyridine bound to the micelle, γ is the angle between the magnetic field and the pyridine molecular director, $\boldsymbol{D}$, and α_i is the angle between the bond to deuteron i and $\boldsymbol{D}$. The brackets indicate an averaging over some anisotropic distribution of pyridine orientations.

These micelles orient with the normal vector for DMPC bilayer perpendicular to the magnetic field (Sanders and Prestegard, 1990; Sanders, 1993; Sanders et al., 1993). Thus, for perfectly oriented micelles, γ is 90° and the expression in γ reduces to −1. In reality, the micelles do not attain perfect order, and this average over γ is represented by the produce of the ideal value and an order parameter, S_γ, that falls between 1 (perfect order) and 0 (isotropic behavior). Values of

S_γ for the DMPC/Triton X-100 micelles are given in Table 1 as described above. Because there is no macroscopic order about this normal vector, the molecular director for pyridine bound to the DMPC domain will necessarily be parallel to the bilayer normal.

The cos α_i terms in Eq. 6 can be defined by the dot product between $\boldsymbol{D}$ and a unit vector coincident with the bond, $\boldsymbol{B}_i$. This can be expanded in the form

$$\cos\alpha_i = \sin\theta_i\cos\phi_i\sin\theta_D\cos\phi_D + sin\,\theta_i\sin\phi_i\sin\theta_D\sin\phi_D + \cos\theta_i\cos\theta_D, \quad (7)$$

where θ_i, ϕ_i are the polar coordinates of $\boldsymbol{B}_i$ and θ_D, ϕ_D are those of $\boldsymbol{D}$ in the pyridine frame of reference. The latter was chosen with the z axis perpendicular to the pyridine ring and the x axis parallel to the para-deuteron bond. Given this definition, all θ_i are 90° and the last term in the sum is zero.

The two ortho deuterons are experimentally indistinguishable and so are the two meta deuterons, which is equivalent to a direct average of director orientations with ϕ_D and $-\phi_D$. Given these considerations, Eq. 6 takes on the form

$$\Delta\nu_i = -3AS_\gamma\sum_j f_j 3[\cos^2\phi_i\langle\sin^2\theta_D\cos^2\phi_D\rangle_j + \sin^2\phi_i\langle\sin^2\theta_D\sin^2\phi_D\rangle_j] - 1\}/8, \quad (8)$$

where the summation in j is over discrete binding sites, e.g., surfactant rim versus lipid bilayer, and the ϕ_i values are $\phi_{para} = 0°$, $\phi_{meta} = 62.2°$, and $\phi_{ortho} = 123.9°$ using the structure of pyridine determined from microwave spectroscopy (Sørensen et al., 1974).

Assuming θ_D and ϕ_D vary independently, the averages indicated by the brackets can be expressed as

$$\langle\sin^2\theta_D\cos^2\phi_D\rangle = \frac{\int\sin^2\theta P(\theta)\sin\theta\,d\theta\int\cos^2\phi P(\phi)\,d\phi}{\int P(\theta)\sin\theta\,d\theta\int P(\phi)\,d\Phi} \quad (9a)$$

$$\langle\sin^2\theta_D\sin^2\phi_D\rangle = \langle\sin^2\theta_D\rangle - \langle\sin^2\theta_D\cos^2\phi_D\rangle \quad (9b)$$

$$\langle\sin^2\theta_D\rangle = \frac{\int\sin^2\theta P(\theta)\sin\theta\,d\theta}{P(\theta)\sin\theta\,d\theta}, \quad (9c)$$

where the integrals in θ are from 0 to π, ϕ is from 0 to 2π, and $P(\theta)$ and $P(\phi)$ are the distribution functions for the two variables, which depend on the details of the local environment of the binding site.

Equations 8 and 9 can be rearranged to yield expressions for $\langle\sin^2\theta_D\rangle$ and $\langle\cos^2\phi_D\rangle$ in terms of the measured splittings, f calculated from the para-deuteron splittings as described above, S_γ from the ^{13}C chemical shifts, and 185 kHz for the quadrupolar coupling constant (Abe and Yamazaki, 1989). Because the signs on the quadrupolar splittings are not known, these relations yield multiple possible solutions for these two average quantities; however, all values must fall between zero and positive unity. Considering all possible combinations of signs on the splittings in Table 4 yields two sets of solutions: $\langle\sin^2\theta_D\rangle = 0.48 \pm 0.02$ with $\langle\cos^2\phi_D\rangle = 0.96 \pm 0.02$ or 0.42 ± 0.02, and $\langle\sin^2\theta_D\rangle = 0.85 \pm 0.01$ with $\langle\cos^2\phi_D\rangle = 0.54 \pm 0.02$ or 0.24 ± 0.02.

To estimate the polar coordinates of the molecular director, it is necessary to consider the expressions for the averages given in Eq. 9. The exact forms of $P(\theta)$ and $P(\phi)$ will depend on the details of the local environment, which are not known. Even if it is assumed that they are Gaussian distributions, there is insufficient information to determine both the average angles and the widths of the distributions. Fig. 6*A* presents plots of $\langle\sin^2\theta_D\rangle$ versus average θ_D, calculated by numerically integrating Eq. 9c using a Gaussian form for $P(\theta)$ and SDs in θ_D of 18°, 9°, and 2°. For this range of SDs, the two values of $\langle\sin^2\theta_D\rangle$ from the splittings correspond to θ_D of 36°–44° and 68°–72°. The former would be consistent

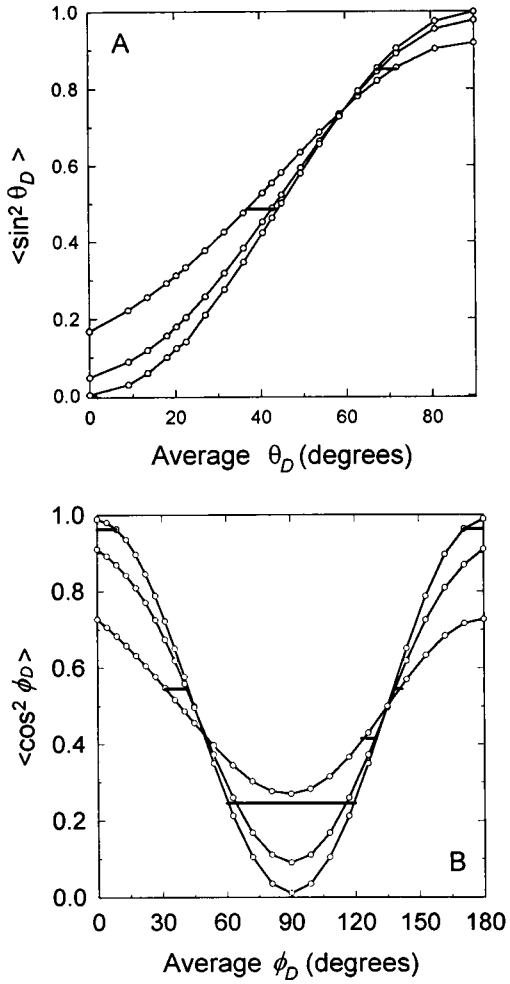

FIGURE 6 Estimation of average values for θ_D and ϕ_D assuming Gaussian distributions. (*A*) Integrated values for $\langle\sin^2\theta_D\rangle$ vs. average θ_D. At $\theta_D = 0°$, the curves from top to bottom are for SDs in the distribution of 18°, 9°, and 2°. The two horizontal lines correspond to the two experimental values: $\langle\sin^2\theta_D\rangle = 0.48$ ($36° < \theta_D < 44°$) and $\langle\sin^2\theta_D\rangle = 0.85$ ($68° < \theta_D < 72°$). (*B*) Integrated values for $\langle\cos^2\phi_D\rangle$ vs. average ϕ_D. At $\phi_D = 0°$ the curves from top to bottom are 6°, 18°, and 36°. The horizontal lines correspond to the experimental values of $\langle\cos^2\phi_D\rangle$, which for $\langle\sin^2\theta_D\rangle = 0.48$ are $\langle\cos^2\phi_D\rangle = 0.96$ ($-9° < \phi_D < +9°$) and 0.42 ($50° < \phi_D < 51°$ or $123° < \phi_D < 130°$) and for $\langle\sin^2\theta_D\rangle = 0.85$ are $\langle\cos^2\phi_D\rangle = 0.54$ ($32° < \phi_D < 41°$ or $138° < \phi_D < 142°$) and 0.24 ($60° < \phi_D < 120°$).

with the orientation of pyridine expected in the headgroup region, whereas the latter is more consistent with the tilt of the acyl chains (Hauser et al., 1988).

The same approach was used to generate the plots of $\langle\cos^2\phi_D\rangle$ vs. ϕ_D presented in Fig. 6 *B* with the experimental estimates of $\langle\cos^2\phi_D\rangle$ displayed as horizontal bars to indicate the possible ranges of ϕ_D for each θ_D range. Values for ϕ_D are given in the figure caption. Broader distributions were used in constructing the $\langle\cos^2\phi_D\rangle$ curves because variation in ϕ_D should be less restricted by the local environment, i.e., greater resistance is expected in tipping the ring (θ_D) than in rotating within the plane of the ring (ϕ_D).

DISCUSSION

Phospholipid membranes present local environments that change drastically in local polarity and order, proceeding from the aqueous interface to the hydrophobic center. There is a general increase in molecular order proceeding from the aqueous phase through the headgroup region and a few carbons down the acyl chain, beyond which there is a decrease in order down the remaining length of the acyl chains (Pope and Dubro, 1986; Boden et al., 1988; Boden et al., 1991). As a result of these features, the bilayer can accommodate included species in various ways (De Young and Dill, 1988; Jacobs and White, 1989; Sanders and Schwonek, 1993; Bassilino-Klimas et al., 1993; Xiang and Anderson, 1994), with correspondingly variable consequences in the phase characteristics of the membrane (Mountcastle et al., 1978; Pope and Dubro, 1986; Makriyannis et al., 1986; Boden et al., 1988; Gaillard et al., 1991; Jørgensen et al., 1993). Small amphiphiles are expected to collect in the glycerol and headgroup regions as a matter of reducing interfacial tension of the membrane and because the lipid headgroups are loosely packed, easily accommodating the added bulk of the amphiphile. The details of these associations are important in testing current models and simulations of solute-membrane interactions (De Young and Dill, 1988; Jacobs and White, 1989; Sanders and Schwonek, 1993; Bassilino-Klimas et al., 1993; Xiang and Anderson, 1994), which in turn are essential in deciphering the relations between the membrane phase properties and biological activity.

Pyridine was chosen to probe the membrane environment readily accessible to small amphiphiles because it is aromatic, rigid, and has three chemically distinct positions on the ring from the standpoint of NMR. Ring current shifts of the ^{13}C resonances for DMPC place pyridine in close contact with both the choline and glycerol groups of the lipid, the same location proposed for benzyl alcohol based on perturbations of ^2H order parameters for the lipid (Boden et al., 1988). The principal difference between the two amphiphiles is that benzyl alcohol can hydrogen-bond to the phosphate moiety, whereas pyridine at pH 9 can not. This pH was chosen to avoid the complications of the cationic pyridinium ion (pK_a = 5.19; Windholz, 1983) binding to a neutral surface, i.e., double layer effects in the binding equilibrium and changes in pK_a for the absorbed pyridinium.

Pyridine causes an increase in the peak heat capacity and a decrease in temperature for the main transition of DMPC (Fig. 1). This is indicative of an amphiphile that is displaced to some extent upon forming the $P_{\beta'}$ gel-state (Jørgensen et al., 1993). The ^2H NMR spectrum of d_5-pyridine in DMPC liposomes exhibits an increase in quadrupolar splitting as the temperature is lowered through the transition temperature (Table 2). Therefore, there must be a substantial level of pyridine still bound to the gel-state, but in a much more restricted environment than in the fluid state. The pretransition decreases in temperature and area with added pyridine and broadens significantly (Fig. 1). Broadening of this transition would be consistent with pyridine bound in the $P_{\beta'}$ state remaining in the interface as the $L_{\beta'}$ forms. This is consistent with the persistence, and even increase, of the d_5-pyridine quadrupolar splittings when the temperature is dropped to 10°C.

At 10:1 pyridine:DMPC (40°C), approximately 70% of the liposome surface sites are occupied by pyridine. Because pyridine has virtually no effect on the ^{31}P CSA of the lipid, indicating little perturbation of the phosphodiester groups, it must partition into a relatively free volume within the interface. There are 8–10 water molecules per phosphatidylcholine hydrating the interface of the gel phase (Wiener et al., 1989), with a greater number expected in the liquid crystalline state. Some of the water associated with the membrane is motionally restricted, as is clearly indicated by the appearance of ^2H quadrupolar splitting for ^2H_2O in liposome suspensions (Finer, 1973; Gawrisch et al., 1992). Displacement of this water by pyridine should result in a concomitant decrease in the ^2H_2O quadrupolar splitting; however, the converse is observed (Table 1). The increase in ^2H_2O splitting indicates that not only is this restricted water not displaced, but pyridine either restricts its motion further or increases the amount of water that is in regions of high order. The latter was observed in neutron diffraction studies of hydrophobic tripetides binding to DMPC vesicles (Jacobs and White, 1989).

DMPC/surfactant micelles were investigated as an alternative to liposome suspensions for NMR studies of amphiphile-membrane associations. These oriented micelles retain much of the resolution and sensitivity of a high resolution NMR experiment while providing new spectral features that are useful in structural studies, such as quadrupolar and dipolar couplings. The disadvantage with these micelles is that there are two distinct domains into which the amphiphile can partition. d_5-Pyridine appears to bind to both the surfactant and phospholipid domains with DMPC/CHAPSO micelles, as evidenced by changes in the ratios of quadrupolar splittings, $\Delta\nu_o/\Delta\nu_p$ and $\Delta\nu_m/\Delta\nu_p$, with increasing DMPC content (Table 3). These splitting ratios are sensitive only to the average local environment of the amphiphile bound to the micelles. As the DMPC level is increase, the values for $\Delta\nu_o/\Delta\nu_p$ and $\Delta\nu_m/\Delta\nu_p$ approach those observed for d_5-pyridine bound to DMPC multilamellar liposomes (Tables 2 and 4). This confirms that the pyridine shifts to the phospholipid domain with increasing DMPC where it has a

local environment comparable to that of pure DMPC liposomes. The splitting ratios for pyridine in DMPC/Triton X-100 micelles are relatively invariant with DMPC content and are always comparable with those of pyridine in DMPC multilamellar liposomes (Tables 2 and 4), suggesting that pyridine preferentially associates with the phospholipid domain in these micelles.

The purpose in using magnetically oriented micelles was to provide better resolution and sensitivity for measuring the quadrupolar splittings of the associated amphiphile. These splittings provide the means to characterize the average orientation of the molecule in the bilayer, which is necessary for any test of molecular dynamics simulations of the amphiphile in the bilayer. Because pyridine is planar, it is necessary to know the micelle order parameter and the fraction bound to the oriented micelles to extract enough information to estimate both $\langle \sin^2 \theta_D \rangle$ and $\langle \cos^2 \phi_D \rangle$, the parameters defining the average orientation.

The micelle order parameter was calculated from ^{13}C chemical shifts according to the work presented by Sanders (1993). The fraction of the pyridine bound to the DMPC/Triton X-100 micelles was estimated from the splitting of the para-deuteron resonances using and the pyridine order parameter from the para-deuteron splitting for pyridine bound to the liposomes and the micelle order parameter. Half as much pyridine appears to bind in the micelle solutions relative to the fraction bound in the liposome suspensions. This may be an indication that some of the pyridine associates with unoriented micelles rich in Triton X-100 that coexist with the oriented species. Characterization of the molecular director requires only the fraction of pyridine bound to the oriented phase, which is the quantity provided by this analysis. Values for $\langle \sin^2 \theta_D \rangle$ and $\langle \cos^2 \phi_D \rangle$ were calculated from the deuterium splittings using these results. However, translation of these quantities to average values for the director coordinates, θ_D and ϕ_D, requires knowledge of the distribution functions for the two averages indicated by the brackets. Assuming Gaussian distributions, plots of $\langle \sin^2 \theta_D \rangle$ vs. average θ_D and $\langle \cos^2 \phi_D \rangle$ vs. average ϕ_D were constructed by numerically integrating the expressions for these averages for several values of the SDs in the distributions (Fig. 6). On the basis of these plots the experimental values for $\langle \sin^2 \theta_D \rangle$ correspond to a θ_D of either $40° \pm 4°$ or $70° \pm 2°$. Each of these has three possible values for ϕ_D (Fig. 6 *B*).

The pyridine aromatic ring would be parallel to the bilayer surface for $\theta_D = 0°$ and perpendicular to the surface for $\theta_D = 90°$. The experimental value of 40° is consistent with the tilt of the ring that might be expected in the head-group and glycerol interface (Hauser et al., 1988), the location suggested by the ^{13}C data. A tilt of 70°, as it is defined here, corresponds to the angle expected for pyridine intercalated among the phospholipid acyl chains (Hauser et al., 1988; Wiener et al., 1989). Both the tighter packing and the ^{13}C chemical shift data argue against this location.

These molecular details are of the kind needed to test the solute behavior in simulations such as that of benzene diffusion in a bilayer (Bassolino-Kilmas et al., 1993). In those simulations, benzene freely diffused throughout the hydrophobic core but may preferentially associate with the carbonyl and terminal methyl regions of the acyl chains. Pyridine and a similar amphiphile, benzyl alcohol (Boden et al., 1988), appear to reside more in the aqueous interface, as expected. The effect of functionality and size of the aromatic group on its localization and orientation in the membrane is the topic of ongoing studies in this laboratory.

The work with the DMPC/surfactant micelles demonstrates a general approach for establishing the conditions under which a substance partitions into the phospholipid domain. The relative ease of sample preparation and the sharp deuterium doublets arising from magnetically ordering the micelles are experimental conveniences that justify this effort. The structural information that can be derived from deuterium NMR studies with these micelles has already been demonstrated with glycolipids (Sanders and Prestegard, 1991; Hare et al., 1993), and there have been similar efforts with deuterated gramicidin in an aqueous decylsulfate/decanol lyotropic liquid crystal (Davis, 1988). Current efforts in this laboratory are focused on applying these methods to conformational studies of peptides in a bilayer environment.

J. M. Henderson was supported by the Nabisco Biscuit Company, R. Iannucci was supported by CIBA-GEIGY Corporation.

REFERENCES

Abe, A, and T. Yamazaki. 1989. Deuterium NMR analysis of poly(γ-benzyl L-glutamate) in the lyotropic liquid-crystalline state: orientational order of the α-helical backbone and conformation of the pendant side chain. *Macromolecules*. 22:2138–2145.

Barry, J. A., and K. Gawrisch. 1994. Direct NMR evidence for surface binding of ethanol to lipid bilayers. *Biophys. J.* 66:386*a*. (Abstr.)

Bassolino-Klimas, D., H. E. Alper, and T. R. Stouch. 1993. Solute diffusion in lipid bilayer membranes: an atomic level study by molecular dynamics simulation. *Biochemistry*. 32:12624–12637.

Bloom, M., J. H. Davis, and A. L. Mackay. 1981. Direct determination of the oriented sample NMR spectrum from the powder spectrum for systems with local axial symmetry. *Chem. Phys. Lett.* 80:198–202.

Boden, N., R. J. Bushby, P. F. Knowles, and F. Sixl. 1988. Partial molecular surface areas as a probe of chemical equilibria in lipid bilayers: anticooperative binding of benzyl alcohol to dimyristoyl phosphatidylcholine. *Chem. Phys. Lett.* 145:315–320.

Boden, N., S. A. Jones, and F. Sixl. 1991. On the use of deuterium nuclear magnetic resonance as a probe of chain packing in lipid bilayers. *Biochemistry*. 30:2146–2155.

Borchard, A., and J. Wolfgang. 1989. The effect of pyridine on the onset lag of photophosphorylation: no evidence for "localized coupling". *Curr. Res. Photosynth., Proc. 8th Int. Conf. Photosynth.* 3:97–100.

Cevc, G. 1991. Isothermal lipid phase transitions. *Chem. Phys. Lipids*. 57: 293–307.

Davis, J. H. 1988. ^2H nuclear magnetic resonance of exchange-labeled gramicidin in an oriented lyotropic nematic phase. *Biochemistry*. 27: 428–436.

De Loof, H., S. C. Harvey, J. P. Segrest, and R. W. Pastor. 1991. Mean field stochastic boundary molecular dynamics simulation of a phospholipid in a membrane. *Biochemistry*. 30:2099–2113.

De Young, L. R., and K. A. Dill. 1988. Solute partitioning into lipid bilayer membranes. *Biochemistry*. 27:5281–5289.

Finer, E. G. 1973. Interpretation of deuterium magnetic resonance spectroscopic studies of the hydration of macromolecules. *J. Chem. Soc. Faraday Trans. II*. 69:1590–1600.

Forrest, B. J., and J. Mattai. 1985. ^{2}H and ^{31}P NMR study of the interaction of general anesthetics with phosphatidylcholine membranes. *Biochemistry*. 24:7148–7153.

Gaillard, S., J.-P. Renou, M. Bonnet, X. Vignon, and E. J. Dufourc. 1991. Halothane-induced membrane reorganization monitored by DSC, freeze fracture electron microscopy and ^{31}P-NMR techniques. *Eur. J. Biophys.* 19:265–274.

Gawrisch, K., D. Ruston, J. Zimmerberg, V. A. Parsegian, R. P. Rand, and N. Fuller. 1992. Membrane dipole potentials, hydration forces, and the ordering of water at membrane surfaces. *Biophys. J.* 61:1213–1223.

Hare, B. J., K. P. Howard, and J. H. Prestegard. 1993. Torsion angle analysis of glycolipid order at membrane surfaces. *Biophys. J.* 64:392–398.

Hauser, H., I. Pascher, and S. Sundell. 1988. Preferred conformation and dynamics of the glycerol backbone in phospholipids. An NMR and X-ray single-crystal analysis. *Biochemistry*. 27:9166–9174.

Henderson, H. M., N. A. Eskin, C. Pinsky, R. Bose, and A. M. Ahique. 1992. Pyridine and other coal tar constituents as inhibitors of potato polyphenol oxidase: a non-animal model for neurochemical studies. *Life Sci.* 51: PL207–PL210.

Ishihara, M., T. Tsuneya, M. Shiga, S. Kawashima, K. Yamagishi, F. Yoshida, H. Sato, and K. Uneyama. 1992. New pyridine derivatives and basic components in spearmint oil (*Mentha gentilis f. cardiaca*) and peppermint oil (*Menta piperita*). *J. Agric. Food Chem.* 40:1647–1655.

Jacobs, R. E., and S. H. White. 1989. The nature of the hydrophobic binding of small peptides at the bilayer interface: implications for the insertion of transbilayer helices. *Biochemistry*. 28:3421–3437.

Jørgensen, K., J. H. Ipsen, O. B. Mouritsen, and M. J. Zuckermann. 1993. The effect of anaesthetics on the dynamic heterogeneity of lipid membranes. *Chem. Phys. Lipids*. 65:205–216.

Kim, H., S. G. Kim., M. Y. Lee, and R. F. Novak. 1992. Evidence for elevation of cytochrome P4502E1 (alcohol-inducible form) mRNA level in rat kidney following pyridine administration. *Biochem. Biophys. Res. Commun.* 186:846–853.

Lipnick, R. L. 1989. A quantitative structure-activity relationship study of Overton's data on the narcosis and toxicity of organic compounds to the Tadpole, *Rana temporaria*. *In* Aquatic Toxicology and Environmental Fate: Eleventh Volume, ASTM STP 1007. G. W. Suter II and M. A. Lewis, editors. American Society for Testing and Materials, Philadelphia. 468–489.

Mabrey, S., and J. M. Sturtevant. 1976. Investigation of phase transitions of lipids and lipid mixtures by high sensitivity differential scanning calorimetry. *Proc. Natl. Acad. Sci. USA*. 73:3862–3866.

Makriyannis, A., D. J. Siminovitch, S. K. Gupta, and R. G. Griffin. 1986. Studies on the interaction of anesthetic steroids with phosphatidylcholine using ^{2}H and ^{13}C solid state NMR. *Biochim. Biophys. Acta*. 859:49–55.

Mountcastle, D. B., R. L. Biltonen, and M. J. Halsey. 1978. Effect of anesthetics and pressure on the thermotropic behavior of multilamellar dipalmitoylphosphatidylcholine liposomes. *Proc. Natl. Acad. Sci. USA*. 75: 4906–4910.

Murari, R., M. P. Murari, and W. J. Baumann. 1986. Sterol orientations in phosphatidylcholine liposomes as determined by deuterium NMR. *Biochemistry*. 25:1062–1067.

Pastor, R. W., R. M. Venable, and M. Karplus. 1991. Model for the structure of the lipid bilayer. *Proc. Natl. Acad. Sci. USA*. 88:892–896.

Pinsky, C., and R. Bose. 1988. Pyridine and other coal tar constituents as free radical-generating environmental neurotoxicants. *Mol. Cell. Biochem.* 84:217–222.

Pope, J. M., and D. W. Dubro. 1986. The interaction of n-alkanes and n-alcohols with lipid bilayer membranes: a ^{2}H-NMR study. *Biochim. Biophys. Acta*. 858:243–253.

Ram, P., and J. H. Prestegard. 1988. Magnetic field induced ordering of bile salt/phospholipid micelles: new media for NMR structural studies. *Biochim. Biophys. Acta*. 940:289–294.

Renou, J.-P., J. B. Giziewicz, I. C. P. Smith, and H. C. Jarrell. 1989. Glycolipid membrane surface structure: orientation, conformation and motion of a disaccharide headgroup. *Biochemistry*. 28:1804–1814.

Sanders, C. R. II. 1993. Solid state ^{13}C NMR of unlabeled phosphatidylcholine bilayers: spectral assignments and measurement of carbon-phosphorous dipolar couplings and ^{13}C chemical shift anisotropies. *Biophys. J.* 64:171–181.

Sanders, C. R. II, and J. H. Prestegard. 1990. Magnetically orientable phospholipid bilayers containing small amounts of bile salt analogue, CHAPSO. *Biophys. J.* 58:447–460.

Sanders, C. R. II, and J. H. Prestegard. 1991. Orientation and dynamics of β-dodecyl glucopyransoside in phospholipid bilayers by oriented sample nmr and order matrix analysis. *J. Am. Chem. Soc.* 113:1987–1996.

Sanders, C. R. II, and J. H. Prestegard. 1992. Headgroup orientation of alkyl glycosides at a lipid bilayer interface. *J. Am. Chem. Soc.* 114:7096–7107.

Sanders, C. R. II, J. A. Schaff, and J. H. Prestegard. 1993. Orientational behavior of phosphatidylcholine bilayers in the presence of aromatic amphiphiles and a magnetic field. *Biophys. J.* 64:1069–1080.

Sanders, C. R. II, and J. P. Schwonek. 1993. An approximate model and empirical energy function for solute interactions with a water phosphatidylcholine interface. *Biophys. J.* 65:1207–1218.

Seelig, J. 1978. ^{31}P nuclear magnetic resonance and the head group structure of phospholipids in membranes. *Biochim. Biophys. Acta*. 515:105–140.

Shimoda, M., and T. Shibamoto. 1990. Isolation and identification of headspace volatiles from brewed coffee with an on-column GC/MS method. *J. Agric. Food Chem.* 38:802–804.

Sørensen, G. O., L. Mahler, and N. Rastrup-Andersen. 1974. Microwave spectra of [^{15}N] and [^{13}C] pyridines, quadrupolar coupling constants, dipole moment and molecular structure of pyridine. *J. Mol. Struct.* 20: 119–126.

Tsukioka, T., and T. Murakami. 1987. Capillary gas chromatographic-mass spectrometric determination of pyridine bases in environmental samples. *J. Chromatogr.* 396:319–326.

Ulmius, J., H. Wennerström, G. Lindblom, and G. Arvidson. 1977. Deuteron nuclear magnetic resonance studies of phase equilibria in a lecithin-water system. *Biochemistry*. 16:5742–5745.

Venable, R. M., Y. Zhang, B. J. Hardy, and R. W. Pastor. 1993. Molecular dynamics simulations of a lipid bilayer and of hexadecane: An investigation of membrane fluidity. *Science*. 262:223–226.

Watts, A., and P. J. R. Spooner. 1991. Phospholipid phase transitions as revealed by NMR. *Chem. Phys. Lipids*. 57:195–211.

Wiener, M. C., R. M. Suter, and J. F. Nagle. 1989. Structure of the fully hydrated gel phase of dipalmitoylphosphatidylcholine. *Biophys. J.* 55: 315–325.

Windholz, M., editor. 1983. The Merck Index, Tenth Edition. Merck & Co., Inc. 1149.

Xiang, T.-X., and B. D. Anderson. 1994. Molecular distributions in interphases: statistical mechanical theory combined with molecular dynamics simulation of a model lipid bilayer. *Biophys. J.* 66:561–573.

Yang, D.-P., T. Mavromoustakos, K. Beshah, and A. Makriyannis. 1992. Amphipathic interactions of cannabinoids with membranes. A comparison between Δ^{8}-THC and its *O*-methyl analog using differential scanning calorimetry, X-ray diffraction and solid state ^{2}H-NMR. *Biochim. Biophys. Acta*. 1103:25–36.